Rod Sensitivity, Cone Sensitivity, and Photoreceptor Layer Thickness in Retinal Degenerative Diseases

David G. Birch,[1,2] *Yuquan Wen,*[1] *Kelly Locke,*[1] *and Donald C. Hood*[3]

Purpose. To evaluate the effects of selective rod and/or cone loss on frequency-domain optical coherence tomography (fdOCT) measures of photoreceptor structure in patients with retinal degenerative diseases.

Methods. Six patients with cone dystrophy (CD) and eight patients with retinitis pigmentosa (RP) were recruited from the Southwest Eye Registry on the basis of diagnosis and ERG findings. fdOCT horizontal line scans were segmented to obtain the thicknesses of the outer segments plus RPE (OS+) and the outer nuclear layer (ONL). The normalized product ONL*OS was obtained after dividing by mean ONL*OS values of 23 normal individuals. Visual field sensitivity profiles were obtained with a modified retinal perimeter, from the horizontal midline with short- and long-wave stimuli under dark- and light-adapted conditions.

Results. Patients with CD and normal rod-mediated sensitivity, but decreased cone-mediated sensitivity, showed normal ONL*OS outside the fovea. The total receptor layer was thinned in the fovea, consistent with loss in cone nuclei and Henle's fiber layer. Patients with RP and sensitivity in the dark that was mediated by cones showed ONL*OS thickness that was linearly related to cone sensitivity. ONL*OS thickness was linearly related to rod sensitivity in regions with greater loss of cone than rod sensitivity.

Conclusions. Both rods and cones can support an intact IS/OS junction and normal photoreceptor thickness measures. The product of ONL and OS thicknesses is proportional to the sensitivity mediated by the less abnormal type of photoreceptor. (*Invest Ophthalmol Vis Sci.* 2011;52:7141–7147) DOI:10.1167/iovs.11-7509

High-resolution frequency domain optical coherence tomography (fdOCT) provides remarkable detail of the various layers of the human retina. Of particular importance to the study of retinal degenerative diseases (RDDs) is the capacity to quantify decreases in photoreceptor outer segment (OS) thickness and decreases in outer nuclear layer (ONL) thickness. The accuracy and repeatability of these measures[1] raise the possibility that fdOCT parameters could be useful outcome measures for clinical trials in RDDs. First, however, it is important to understand exactly how fdOCT parameters relate to traditional measures of visual function.

Previous studies have established that the diameter of the highly reflective inner segment/outer segment (IS/OS) junction correlates with the diameter of the visual field in patients with retinitis pigmentosa (RP).[2–4] Within the healthier central region, the photoreceptor layer is typically thinner than in normal subjects, due to both shortening of outer segments (OS) and loss of cells within the outer nuclear layer (ONL).[5] There is considerable variation among patients. For example, a subset of patients with autosomal recessive RP shows normal retinal structure in the central retina, coinciding with normal rod and cone sensitivity.[6] Other patients show decreased thickness in the photoreceptor layer of the central retina related to decreased cone sensitivity.[7–9] A simple linear model[7,10] assumes that visual sensitivity is proportional to the product of the number of surviving photoreceptors and the length of their outer segments. We recently reported that a decrease in the product of ONL thickness and OS thickness correlates with a decrease in cone sensitivity, and this relationship follows the prediction of the simple linear model.[7]

What is not known from previous work is the degree to which fdOCT changes reflect a loss in rod sensitivity in RDDs. We know from histology that peripheral rod OS interdigitate with the RPE and are visibly longer than peripheral cones.[11] On ultrahigh-resolution OCT, distinct subtle bands have been associated with cone OS tips and more distal rod OS tips[12]; but how is the thinning of the ONL and OS layers related to rod, as opposed to cone, sensitivity? To further evaluate the relative effects of rod and cone loss on fdOCT measures of photoreceptor structure, we recruited patients with cone dystrophy (CD) and RP with various degrees of rod- versus cone-mediated functional loss. To relate rod and cone function to fdOCT parameters, we used a modified form of fundus perimetry with direct fundus visualization and spectral stimuli (Crossland M, et al. *IOVS* 2010;51:ARVO E-Abstract 3640). Our goal was to relate rod and cone sensitivity to fdOCT parameters at corresponding locations across the horizontal meridian of these patients.

Methods

All procedures adhered to the tenets of the Declaration of Helsinki, and the Institutional Review Board of UT Southwestern Medical Center approved the study. Written informed consent was obtained from all patients and controls after the procedures and possible consequences were explained.

Patients

Study participants included 6 patients with CD, 8 patients with RP, and 23 normal individuals. Patients without cystoid macula edema (CME), myopia >6 D, or lens opacities above LOCS grade 2 were selected from the database of the Southwest Eye Registry. Patients with CD were selected who had clear evidence of progressive cone loss and normal or near-normal rod ERG amplitudes. Patients incapable of steady fixa-

From the [1]Retina Foundation of Southwest, Dallas, Texas; the [2]Department of Ophthalmology, University of Texas, Southwestern Medical Center, Dallas, Texas; and [3]Department of Psychology, Columbia University, New York, New York.

Supported by National Eye Institute Grant EY 09076 and The Foundation Fighting Blindness.

Submitted for publication March 5, 2011; revised May 26 and July 18, 2011; accepted July 18, 2011.

Disclosure: **D.G. Birch**, None; **Y. Wen**, None; **K. Locke**, None; **D.C. Hood**, None

Corresponding author: David G. Birch, Retina Foundation of Southwest, 9900 N. Central Expressway, Suite 400, Dallas, TX 75231; dbirch@retinafoundation.org.

tion, or with geographic atrophy within the macula, were also excluded. Patients with RP were selected who had detectable cone amplitudes to 31-Hz flicker and measurable field sensitivity throughout most of the central 30°. From this subgroup, we selected patients retaining rod ERG amplitudes ranging from relatively large (15.9 μV) to nondetectable (<2.0 μV). Mutation screening is under way for these patients; to date, mutations have been identified only in patient 652 (*RHO* and *P23H*).

Visual Function

Photopic perimetric sensitivity was measured with spot size 3 (0.86° in diameter) on a Humphrey field analyzer (HFA II; Carl Zeiss Meditec, Inc., Dublin, CA), using the central 30-2 threshold program. Foveal sensitivity was measured in all patients. Total deviation (TD_{HFA}), the difference in decibels at any given location for the patient from that of the age-matched normative database, was used in the analysis.

Scotopic sensitivity was measured after pupil dilation and 45 minutes of dark adaptation on a Goldmann-Weekers dark adaptometer (Haag-Streit, Bern, Switzerland). The test target was an 11° diameter achromatic central spot of 200-ms duration. The mean threshold for each patient was the average of five ascending and five descending determinations. Total deviation (TD_{G-W}) was the difference in decibels between the patient's mean threshold and age-adjusted mean normal threshold.

Fundus perimetry was obtained under dark- and light-adapted conditions on a perimeter (MP-1; NAVIS software, ver. 1.7; Nidek Technologies, Padova, Italy) with a spot size 5 test (3.44° diameter). The MP-1 was modified by adding a filter holder in the stimulus path, providing convenient access to the filter and light-sealing the device (Crossland M, et al. *IOVS* 2010;51:ARVO E-Abstract 3640). After pupil dilation, patients and normal subjects were dark adapted for 30 minutes. Setup and practice took 15 minutes, and so a total of 45 minutes of dark adaption preceded the initiation of data collection. Fundus-guided perimetric sensitivity (with infrared illumination of the fundus) was determined at 2° spacing along the horizontal midline. Sensitivity was first determined with a short-pass filter ($\lambda_{50\%\ cutoff}$ = 502 nm "blue"; NT30-635; Edmund Optics, Barrington, NJ). A neutral-density filter of up to 2.0 ND was added, to adjust to the sensitivity range of the normal subjects and patients, leading to a dynamic range of 40 dB. Next, a second field was obtained at exactly the same locations (using the MP-1 retinal location tracking capability) with a long-pass filter ($\lambda_{50\%\ cut\text{-}on}$ = 590 nm "red"; NT30-634; Edmund Optics). The patient was then light adapted for 10 minutes, and sensitivity to red was remeasured at the same locations under controlled light-adapted conditions (34 cd/m^2).

The TD under dark-adapted condition (TD_{dark}) was derived by subtracting the mean normal value for the blue stimulus from that of the patient. Similarly, the light-adapted value (TD_{light}) was derived from the difference, in decibels, between the patient value and mean normal sensitivity to the red stimulus.

Optical Coherence Tomography

Line scans of the horizontal midline and volume scans of the central retina were obtained with fdOCT (Spectralis HRA+OCT; Heidelberg Engineering, Heidelberg, Germany). The confocal scanning laser ophthalmoscope (cSLO) system provides infrared reflectance (IR; 820 nm) imaging. Optical resolution is approximately 10 μm. The fdOCT runs simultaneously with the cSLO imaging system, using a second, independent pair of scanning mirrors. The wavelength of the fdOCT imaging system is 870 nm. Using high-resolution settings and automated tracking (ART), optical resolution is approximately 7 μm in depth and 15 μm, transversely. Results from the 14 patients were compared to data from 23 individuals with normal findings in eye examinations.[5]

The images of a scan through the fovea were exported to data-analysis software (Igor Pro; WaveMetrics, Inc., Portland, OR) and segmented to identify three boundaries. These were: BM/choroid, the boundary between Bruch's membrane (BM) and the choroid; IS/OS, the border between the inner segment (IS) and outer segment (OS) of the receptors; and INL/OPL, the border between the INL and the outer plexiform layer (OPL).

Using the locations of these boundaries, we defined two retinal regions/layers for comparing patients to controls: The receptor outer segment plus RPE (OS+) is the distance between the IS/OS and BM/choroid boundaries. The outer nuclear layer (ONL) is the distance between INL/OPL and IS/OS boundaries.

We hypothesize that the measured OS+ thickness represents the sum of two components. One component is OS, a measure of the length of the photoreceptor OS. The second component is the residual, or base level *b*, which is primarily RPE, but also has small contributions from the basement membrane and, possibly, the distal tips of

Table 1. Demographics and Clinical Results

Patient ID/Diagnosis	Inheritance	Sex	Age (y)	Rod ERG* (μV)	Cone ERG† (μV)	DA Threshold‡ (TD_{G-W})	Foveal Threshold§ (TD_{HFA})
CD							
9754	Dom	M	44	66.6	14.9	1.7 (−1)	19 (−19)
7190	Isolate	M	11	83.8	6.4	1.7 (−1)	33 (−5)
10102	X-linked	M	48	128	4.5	1.7 (−1)	27 (−11)
10095	Dom	F	61	63.4	<2.0	2.3 (−5)	24 (−12)
3718	Isolate	M	31	43.6	<2.0	2.0 (−4)	24 (−14)
10094	Isolate	F	68	74.2	27.5	2.2 (−4)	33 (−3)
RP							
9990	Isolate	M	41	15.9	2.6	1.5 (0)	34 (−4)
2690	Rec	F	30	14.5	14	3.1 (−15)	31 (−7)
7670	Isolate	M	45	14.2	24.4	2.0 (−4)	30 (−8)
8793	Isolate	M	60	10.1	30.9	2.9 (−13)	31 (−7)
5303	Isolate	F	33	5.7	8.6	3.0 (−14)	38 (0)
7808	Rec	F	59	<2.0	127	4.1 (−25)	37 (−1)
8794	Dom	F	57	<2.0	21.6	1.8 (−2)	37 (−1)
652	Dom	F	62	<2.0	6.6	3.7 (−19)	34 (−2)
Normal limit ≤60				70	35	1.6 (0)	38 (0)
Normal limit >60				50	25	1.8 (0)	36 (0)

* ISCEV (International Society for Clinical Electrophysiology of Vision) single-flash rod response.
† ISCEV single-flash cone response.
‡ Log microapostilbs (TD).
§ dB (TD).

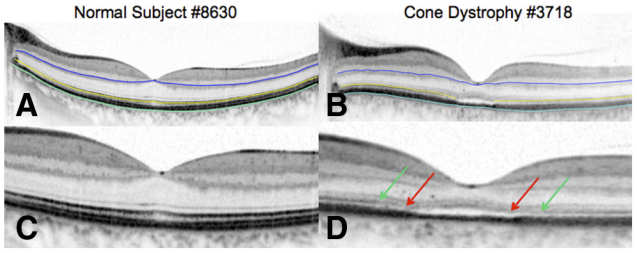

FIGURE 1. Segmented fdOCT scans from horizontal midline. *Light green*: BM/choroid; *yellow*: IS/OS; *blue*: INL/OPL. (**A**) Normal individual. (**B**) Patient 3718 with CD. (**C**) Enlarged image of normal macula. (**D**) Enlarged image of macula in patient3718. *Green arrows*: the point at which the IS/OS line became irregular; *red arrows*: the point at which the IS/OS line disappeared.

the outer segments as well. We set b to 21.5 μm based on the median thickness of OS+ at all locations in patients where field loss was greater than −20 dB (Ref. 7 and confirmed in this study). What we call the ONL also includes the axons (Henle fibers) of the receptors.[13,14] For each patient, we derived the product of OS_j and ONL_j (ONL_j*OS_j) at each location j on the horizontal meridian. Normalized ONL_j*OS_j thickness was obtained by dividing patient ONL_j*OS_j by mean ONL_j*OS_j from normal individuals (n = 23).

Simple Linear Model

A simple linear model was used to relate fdOCT parameters to sensitivity parameters. Specifically, loss of ONL*OS thickness was related to loss of sensitivity in linear, not decibel (i.e., 0.1 log unit) units. Thus, sensitivity in linear terms is $10^{0.1TD}$, and the linear relationship is: normalized ONL*OS = $10^{0.1TD}$. For example, when TD is 0, normalized ONL*OS is 1.0 (normal thickness), when TD is −3 dB, normalized ONL*OS is 0.5 (one-half of normal thickness), and when TD is −10 dB, normalized ONL*OS is 0.1 (one-tenth of normal thickness).

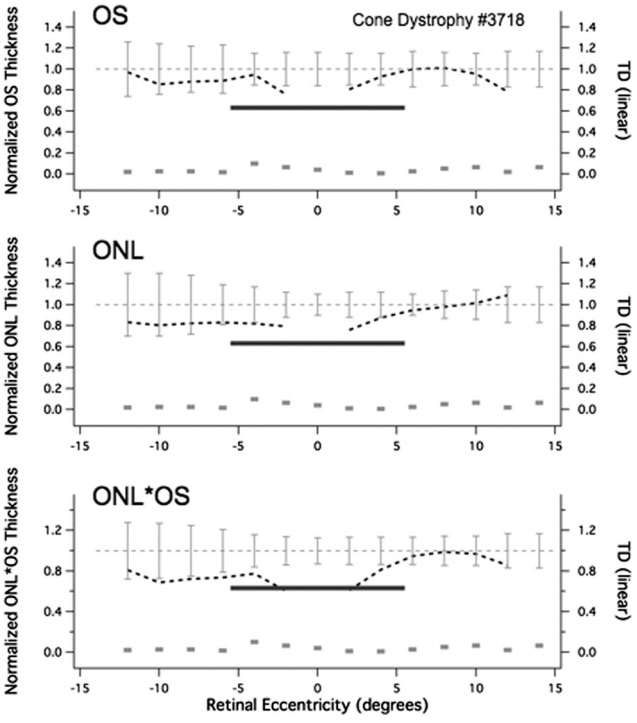

FIGURE 2. Normalized fdOCT parameters plotted against linear TD values for the patient with CD shown in Figure 1. *Dark dashed curve*: normalized fdOCT values; vertical error bars indicate the 95% confidence intervals for normal fdOCT parameters. The gaps in the curves depicting the OS, ONL, and OS*ONL reflect the extent of the loss in the IS/OS junction line in the underlying OCT image (see Fig 1). *Dark gray bars*: $TD_{(G\text{-}W)}$, the linear decrease in rod sensitivity from normal. The length of the bar is 11°, consistent with the diameter of the test target. *Light gray bars*: $TD_{(HFA)}$, the linear decrease in cone sensitivity. Bar lengths are 0.86°, consistent with the diameter of the spot size 3 test target.

RESULTS

Demographics and clinical results from all patients are presented in Table 1. The age (mean ± 1 SD) of patients with CD was 44 ± 21 years, similar to that of patients with RP (48 ± 13 years) and normal controls (36 ± 15 years). Patients with CD had greater cone ERG loss than rod ERG loss. Because of the inclusion criteria, patients with CD showed near normal, rod-mediated, dark-adapted central thresholds ($TD_{G\text{-}W}$ ranged from −1 to −5 dB). Their central retinal cone thresholds were elevated above mean normal in all patients (TD_{HFA} = −10.7; range, −3 to −19 dB).

Patients with RP retained fairly robust cone ERG amplitudes (mean amplitude = 29.5 μV; range, 2.6–127 μV; lower limit of normal = 30 μV), but, because of the selection criteria, showed a range of rod ERG amplitudes from 15.9 μV to nondetectable (<2.0 μV; lower limit of normal = 70 μV). Similarly, rod-mediated, dark-adapted central thresholds showed a range of losses ($TD_{G\text{-}W}$ = −11.5; range, 0 to −25 dB), reflecting the differences in the degree of preserved rod function. On the other hand, the cone elevations were fairly comparable among patients (TD_{HFA} ranged from 0 to −8 dB).

A representative fdOCT scan through the horizontal meridian for normal subject 8630 is shown with segmentation lines superimposed in Figure 1A. The region between the yellow band and the light green band defines OS+. The region between the blue band and the yellow band delineates ONL and includes photoreceptor nuclei, regions of inner segment, and Henle's fiber layer. Figure 1B shows a horizontal scan from patient 3718 with CD. Despite a nondetectable cone ERG, OS+ for this patient is similar to normal at locations outside the fovea, suggesting that rod outer segments alone are sufficient

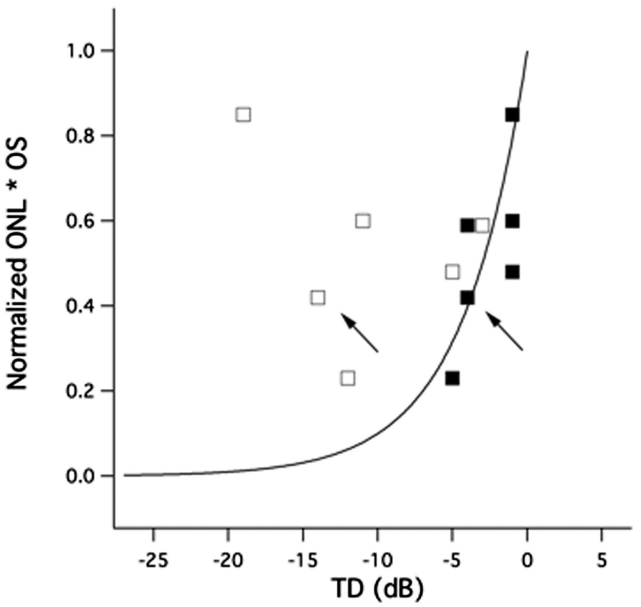

FIGURE 3. Linear relationships between $TD_{G\text{-}W}$ (■), TD_{HFA} (□) and normalized ONL*OS in the macula of CD patient 3718 (*arrows*) and all other patients with CD. The smooth curve is the prediction of a simple linear model,[7] where normalized ONL*OS = $10^{0.1TD}$.

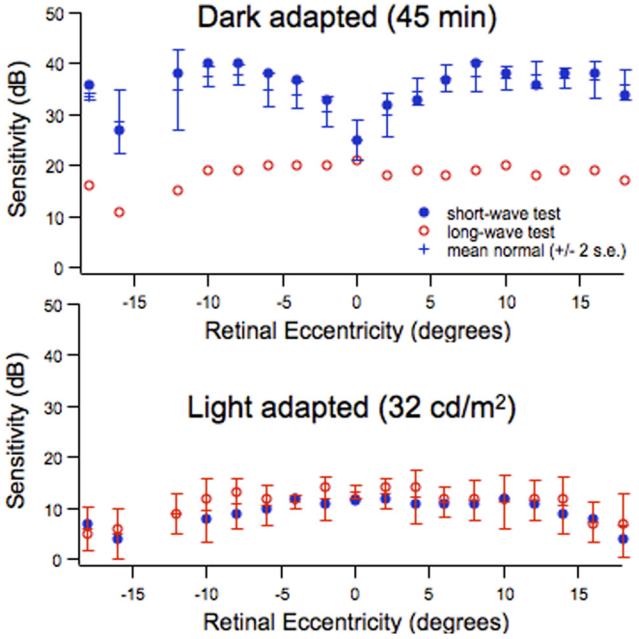

FIGURE 4. *Top*: sensitivity along the horizontal meridian after 45 minutes of dark adaptation. Sensitivity to the short-wave stimulus was higher than sensitivity to the long-wave stimulus at all locations, with an average difference of 18 dB outside the fovea. Vertical bars indicate 95% confidence interval for rod thresholds. *Bottom*: sensitivity along the horizontal meridian after 10 minutes of light adaptation (34 cd/m^2). Sensitivity to the short-wave stimulus was slightly lower than sensitivity to the long-wave stimulus. Vertical bars indicate 95% confidence intervals for cone thresholds.

to preserve normal OS thickness. Figure 1D shows an enlargement of the foveal region. The red arrows indicate where the IS/OS disappears in the fovea, and the green arrows indicate where it starts to break up. Compared to normal (Fig. 1C), the ONL is thinner in the fovea and parafovea, consistent with the loss of foveal cone nuclei and Henle's fiber layer.

The dashed lines in Figure 2 show OS thickness (top), ONL thickness (middle), and ONL*OS thickness (bottom) for the same patient (3718), after dividing thickness in that patient by the mean thickness for 23 normal subjects, to normalize all values. Note that for this patient with CD, values of OS, ONL, and ONL*OS outside the fovea fall within the 95% normal confidence interval (vertical lines). Superimposed on the figures (right *y*-axis) are normalized linear values ($10^{0.1TD}$) for rod-mediated, dark-adapted sensitivity ($TD_{G\text{-}W}$; dark gray bars with length equal to stimulus diameter) and cone-mediated, light-adapted sensitivity (TD_{HFA}; light gray bars equal to stimulus diameter). The normalized thickness of each layer clearly corresponds better to $TD_{G\text{-}W}$ than to TD_{HFA}. This relationship is quantified in Figure 3, which shows the linear relationships between $TD_{G\text{-}W}$, TD_{HFA}, and normalized ONL*OS thickness in the macula for patient 3718 (arrows) and all other patients with CD. The smooth curve is the prediction of a simple linear model[7] proposed in the Methods section (normalized ONL*OS = $10^{0.1TD}$). Note that it is not a straight line, since log values are shown on the *x*-axis. For patients with CD, a simple linear model predicts the relationship between ONL*OS thickness and TD_{GW} (filled squares; $r = 0.81$; $P < 0.05$). However, there is little or no relationship between ONL*OS and TD_{HFA} (open squares; $r = -0.02$; NS).

In contrast to patient 3718, where cone loss appears fairly homogeneous, many patients with CD and most patients with RP have highly heterogeneous rod and cone loss. To measure local variations within the central retina, we obtained rod- and cone-mediated sensitivity profiles across the horizontal meridian with fundus perimetry on the modified perimeter (MP-1; Nidek). The rationale behind the spectral approach is shown for a normal individual in Figure 4. The top panel shows sensitivity along the horizontal meridian after 45 minutes of dark adaptation. Sensitivity to the short-wave stimulus was higher than sensitivity to the long-wave stimulus at all locations, with an average difference of 18 dB outside the fovea. The difference is that predicted for these wavelengths based on the scotopic sensitivity function,[15] indicating that rods detected both stimuli outside the fovea. The smaller difference in the fovea suggests that the cones detected the red stimulus.

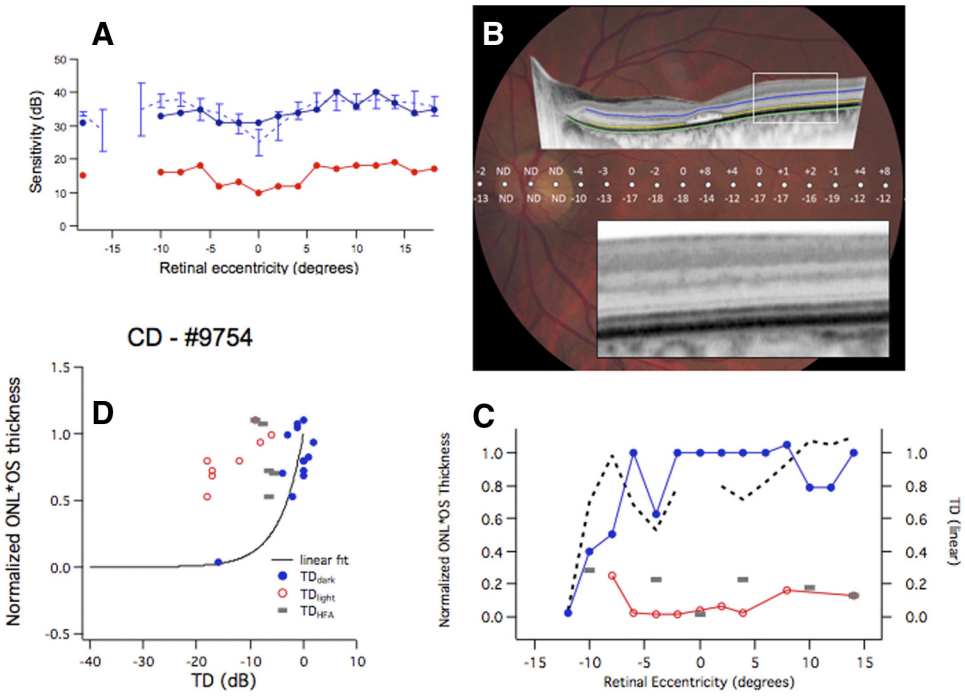

FIGURE 5. fdOCT and MP-1 perimetry in patient 9754 with CD. (**A**) Dark-adapted fundus perimetric sensitivity was higher for blue than for red at all locations, indicating rod mediation of thresholds. (**B**) TD_{dark} and TD_{light} (the difference in decibels between the patient values and mean normal values) are superimposed on a fundus photograph. For comparison, the fdOCT scan is aligned with the perimetric sensitivities. An enlargement is shown of the region indicated by the box. (**C**) Normalized ONL*OS thickness (*dashed curve*, *left axis*), along with rod-mediated TD_{dark} (*filled blue circles*, *right axis*), cone-mediated TD_{light} (*open red circles*) and deviations from Humphrey perimetry (TD_{HFA}, *light gray bars*). Photoreceptor layer thickness is within normal limits outside the fovea, as is TD_{dark} (but not TD_{light}). (**D**) Normalized ONL*OS thickness was consistent with a linear relationship to TD_{dark}.

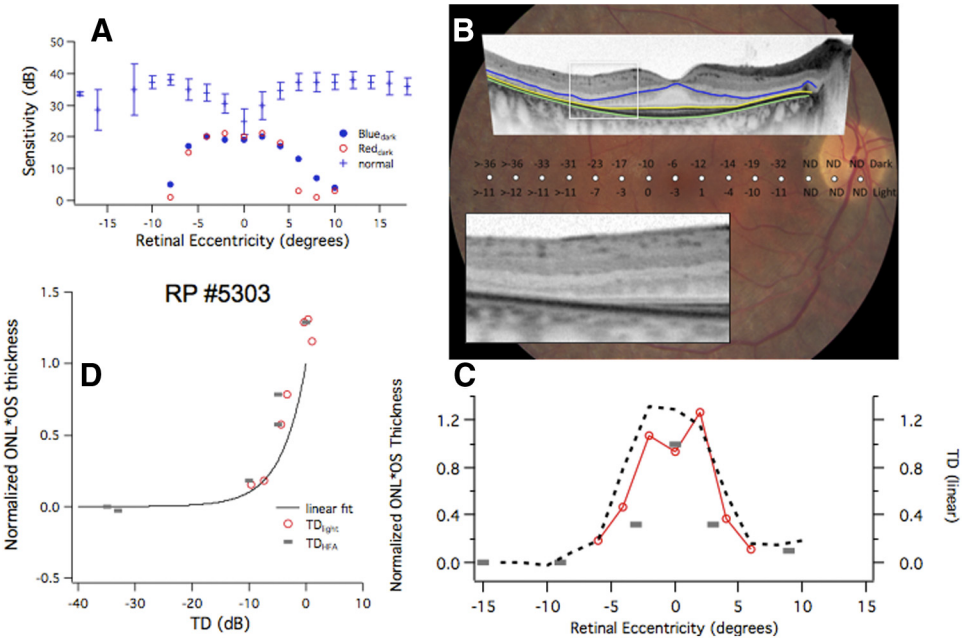

FIGURE 6. FdOCT and MP-1 perimetry in patient 5303 with RP. (**A**) Dark-adapted fundus perimetric sensitivity was similar for blue and red stimuli, consistent with cone mediation of all thresholds. (**B**) TD_{dark} and TD_{light} are superimposed on a fundus photograph. For comparison, the fdOCT scan is aligned with the perimetric sensitivities. An enlargement is shown of the region indicated by the box. (**C**) Normalized ONL*OS thickness (*dashed curve*, *left axis*) is shown, along with linear TD_{dark} (*filled blue circles*, *right axis*), linear TD_{light} (*open red circles*, *right axis*), and linear deviations from Humphrey perimetry (TD_{HFA}, *light gray bars*, *right axis*). (**D**) A simple linear model predicts the relationship between ONL*OS thickness and TD_{light}.

Figure 4, bottom, shows sensitivity along the horizontal meridian after 10 minutes of light adaptation (34 cd/m^2). Sensitivity to red was slightly higher than sensitivity to blue, consistent with the slightly higher photopic luminance with the red filter and indicating that cones are detecting both stimuli. For a given location in a patient, a blue-red difference of approximately 18 dB implies that rods detected both stimuli (Fig. 4, top), a difference of 0 dB implies cone mediation of both stimuli (Fig. 4, bottom), and an intermediate value suggests that rods are detecting the blue stimulus with cones detecting the red stimulus. Thus the "blue-red" difference can be used to determine whether rods or cones are mediating sensitivity at each location. For locations in a patient that are rod mediated, the sensitivity to blue after dark adaptation gives a measure of rod sensitivity. Thus, in a normal individual, sensitivity at locations outside the fovea is mediated by rods, and the vertical bars in Figure 4, top, show the 95% confidence intervals for seven normal controls. For locations in a patient that are cone mediated, the sensitivity to red after light adaptation gives a measure of cone sensitivity. The vertical bars in Figure 4, bottom, show the 95% normal confidence interval.

Results for patient 9754 with CD are shown in Figure 5. Figure 5A shows that dark-adapted fundus perimetric sensitivity was higher for blue than for red at all locations, indicating rod mediation of threshold. Furthermore, sensitivity to blue (filled blue circles) fell within the normal 95% confidence interval at most retinal locations. The fdOCT scan is shown in comparison to fundus perimetry in Figure 5B. Here, the perimetric values represent the difference (in decibels) between the patient values and mean normal values. The top row

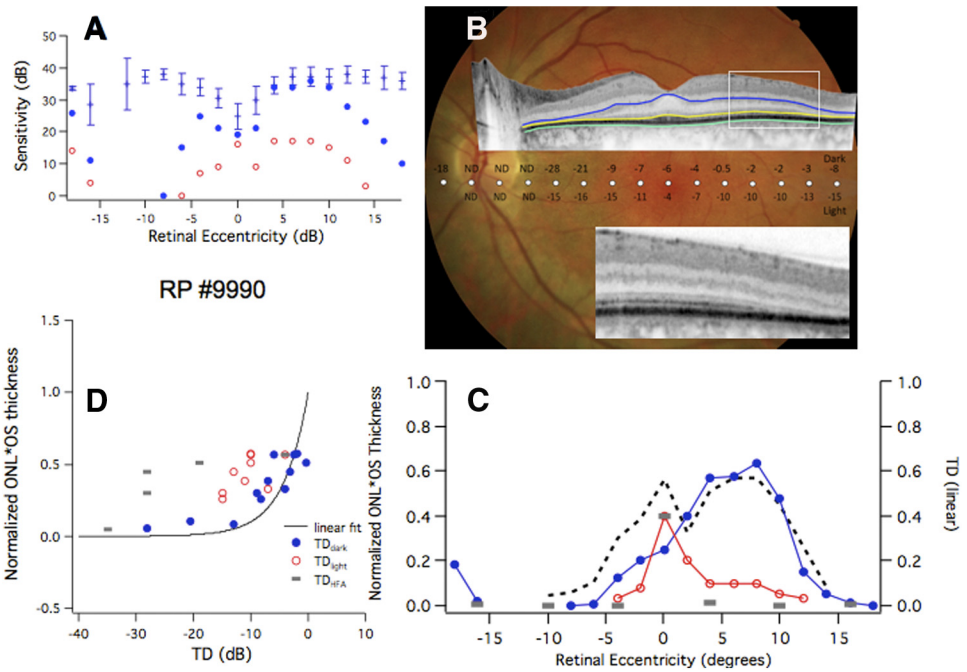

FIGURE 7. FdOCT and MP-1 perimetry in patient 9900 with RP. (**A**) Dark-adapted fundus perimetric sensitivity was higher for *blue* and than for *red* stimuli in the temporal retina, consistent with rod mediation of thresholds. (**B**) The horizontal fdOCT scan is shown along with TD_{dark} and TD_{light}. An enlargement is shown of the region indicated by the box. (**C**) Normalized ONL*OS thickness is shown along with TD_{dark} (*filled blue circles*), TD_{light} (*open red circles*) and TD_{HFA} (*light gray bars*). Foveal thickness corresponds to a peak in TD_{light}, whereas relative ONL*OS thickness in the temporal retina corresponds to relatively normal values of TD_{dark}. (**D**) The simple linear model for ONL*OS thickness (*smooth curve*) provides a better approximation to TD_{dark} than to TD_{light}.

(TD_{dark}) is the deviation for the blue stimulus under dark-adapted conditions; the bottom row (TD_{light}) is the deviation for the red stimulus under light-adapted conditions. It is clear that the rod (dark) threshold was near normal across the field test, whereas the cone (light) sensitivity was depressed by −10 to −18 dB. Normalized ONL*OS thickness is shown in Figure 5C, along with rod-mediated TD_{dark}, cone-mediated TD_{light}, and deviations from Humphrey perimetry (TD_{HFA}). Photoreceptor layer thickness was within normal limits outside the fovea, as was TD_{dark}. However, TD_{light} was below normal at all locations. As shown in Figure 5D, normalized ONL*OS thickness was consistent with a linear relationship to TD_{dark}. However, TD_{light} was not related to normalized thickness.

Results from patient 5303 with RP are shown in Figure 6. Dark-adapted fundus perimetric sensitivity was similar for blue and red stimuli (Fig. 6A), consistent with cone mediation of all thresholds. The horizontal fdOCT scan is shown, along with TD_{dark} and TD_{light} in Figure 6B. Figure 6C shows a good relationship between ONL*OS thickness and TD_{light}. In Figure 6D, it can be seen that the simple linear model predicted the relationship between ONL*OS thickness and TD_{light}.

Results from a second patient with RP, 9990, are shown in Figure 7. Dark-adapted fundus perimetric sensitivity was higher for blue and than for red stimuli in the temporal retina (Fig. 7A), consistent with rod mediation of thresholds. The horizontal fdOCT scan is shown along with TD_{dark} and TD_{light} in Figure 7B. Normalized ONL*OS is shown along with linear TD_{dark}, linear TD_{light}, and linear TD_{HFA} in Figure 7C. Foveal thickness corresponded to a peak in TD_{light}, whereas relative ONL*OS thickness in the temporal retina corresponded to relatively normal values of TD_{dark}. As shown in Figure 7D, the simple linear model for ONL*OS thickness provided a better approximation of TD_{dark} than of TD_{light} for most values.

Four of the eight patients with RP had at least some locations in the central retina where sensitivity was mediated by rods. Figure 8, top, shows the relationship between TD_{dark} and normalized ONL*OS thickness for these rod-mediated locations. The smooth curve is the linear prediction: $ONL*OS = 10^{0.1TDdark}$. For rod-mediated loci in RP, the simple linear model predicts the relationship between ONL*OS thickness and TD_{dark} ($r = 0.86$; $P < 0.00002$).

All eight patients with RP had at least some locations where sensitivity was mediated by cones. Figure 8, bottom, shows the relationship between TD_{light} and normalized ONL*OS thickness for cone-mediated locations. For cone-mediated loci in RP, the simple linear model ($ONL*OS = 10^{0.1TDlight}$) predicts the relationship between ONL*OS thickness and TD_{light} ($r = 0.71$; $P < 0.00001$).

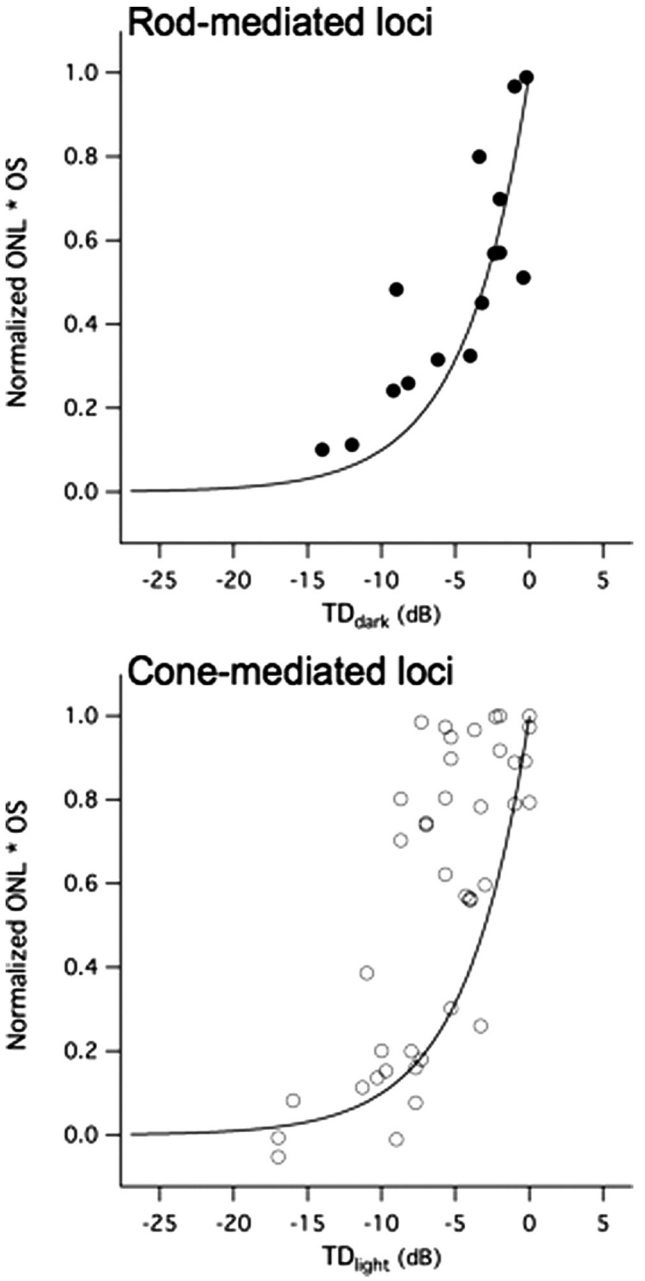

FIGURE 8. Relationship between TD and normalized ONL*OS in RP. *Top*: four of the eight patients with RP had at least some locations in the central retina where sensitivity was mediated by rods. The simple linear model (*solid curve*) predicts the relationship between ONL*OS thickness and TD_{dark}. *Bottom*: all eight patients with RP had at least some locations where sensitivity was mediated by cones. The simple linear model predicts the relationship between ONL*OS and TD_{light}.

DISCUSSION

In a previous study of the correlation between field sensitivity and fdOCT parameters,[7] patients with RP were selected on the basis of visual acuity of at least 20/40, absence of CME, and <6 D of refractive error. Since most patients with RP show early loss of rod function, it is reasonable that OS parameters in that study reflected cone function. Patients with CD and RP were selected for the present study from a large (>2000) database of patients with RDDs and are not necessarily representative. Patients with CD were selected who had relatively normal rod ERG amplitudes, but whose cone ERG amplitude had progressively declined to near nondetectable. Patients with RP were selected who had cone ERG amplitudes averaging 50% of mean normal and a range of rod ERG responses from 25% of mean normal to nondetectable. This select group of patients allowed us to evaluate the relationships among fdOCT measures of photoreceptor thickness and perimetric measures of rod and cone sensitivity.

In patients with CD, OS and ONL thickness was typically within the normal range outside the macula. The product of OS thickness, representing photoreceptor OS length, and ONL thickness, representing photoreceptor density, correlated highly with rod-mediated, dark-adapted visual thresholds. There was no relationship, however, between ONL*OS thickness and cone thresholds. These findings suggest that virtually all cones can be lost without affecting extrafoveal OCT photoreceptor layer thickness. Within the fovea, where cone density is typically highest and rod density is low, fdOCT scans from patients with CD are clearly abnormal. There is no central thickening of the ONL because of the absence of cell bodies

and Henle's fiber layer.[13,14] Frequently, there are foveal spaces, or cavities, similar to those reported previously in achromatopsia and blue-cone monochromacy.[16,17] These may be local foveal detachments due to the loss of cone outer segments in the fovea.

Two-color perimetry, originally pioneered by Wald and Zeavin,[18] was used to map rod and cone thresholds in more detail. Two-color perimetry has previously been used to separate rod and cone function with the Goldmann-Weekers dark adaptometer,[19] the Tübinger perimeter,[20] the Goldmann perimeter,[21] the Humphrey perimeter (Carl Zeiss Meditec),[22] and the Octopus perimeter (Haag-Streit).[15] In the present study, we used the MP-1 fundus perimeter (Nidek). The advantage of the MP-1 is that sensitivity is mapped with direct visualization of the fundus. The MP-1 can correct for poor or eccentric fixation. Since each test is registered using retinal landmarks, sensitivity can be mapped at identical retinal loci on subsequent tests.

The results of two-color fundus perimetry allowed us to determine whether rods mediated the threshold at a given location in patients with CD or RP. In patients like RP 5303 (Fig. 7), in whom there was no evidence of rods within the central 30°, the product of OS and ONL thickness decreased with a decrease in cone-mediated sensitivity and, as shown previously,[7] this decrease followed the prediction of a simple linear model. In other patients such as RP 9990 (Fig. 8), there were locations where ONL*OS thickness and visual thresholds appeared to be determined by rods, whereas foveal sensitivity and thickness was mediated primarily by cones. Across all patients, ONL*OS thickness was linearly related to rod sensitivity at locations where dark-adapted sensitivity was mediated by rods and linearly related to cone sensitivity at locations where dark-adapted sensitivity was mediated by cones. Although the overall correlations were high, many points for cone-mediated loci in Figure 8B fell to the left of the linear fit, suggesting some loss of cone sensitivity before fdOCT thinning.

In screening for participants in this study, we encountered RP patients with normal central rod- and cone-mediated vision in the central retina, along with preserved central retinal structure.[6] These patients were not included in the present study because they did not help distinguish rod versus cone contributions to OCT photoreceptor parameters. It would be interesting, however, to observe such patients over time to determine how ONL*OS thickness is affected as rods degenerate. Such knowledge is crucial before using fdOCT as an outcome measure in clinical trials designed to preserve or restore rods.

References

1. Hood DC, Cho J, Raza AS, Dale EA, Wang M. Reliability of a computer-aided manual procedure for segmenting optical coherence tomography scans. *Optom Vis Sci.* 2011;88:113–123.
2. Fischer MD, Fleischhauer JC, Gillies MC, Sutter FK, Heibig H, Barthelmes D. A. new method to monitor visual field defects caused by photoreceptor by quantitative optical coherence tomography. *Invest Ophthalmol Vis Sci.* 2008;49:3617–3621.
3. Hood DC, Lazow MA, Locke KG, Greenstein VC, Birch DG. The transition zone between healthy and diseased retina in patients with retinitis pigmentosa. *Invest Ophthalmol Vis Sci.* 2011;52: 101–108.
4. Jacobson SG, Aleman TS, Sumaroka A, et al. Disease boundaries in the retina of patients with Usher syndrome caused by MY07A gene mutations. *Invest Ophthalmol Vis Sci.* 2009;50:1886–1894.
5. Hood DC, Lin CE, Lazow MA, Locke KG, Zhang X, Birch DG. Thickness of receptor and post-receptor retinal layers in patients with retinitis pigmentosa measured with frequency-domain optical coherence tomography. *Invest Ophthalmol Vis Sci.* 2009;50: 2328–2336.
6. Jacobson SG, Roman AJ, Aleman TS, et al. Normal central retinal function and structure preserved in retinitis pigmentosa. *Invest Ophthalmol Vis Sci.* 2010;51:1079–1085.
7. Rangaswamy NV, Patel HM, Locke KG, Hood DC, Birch DG. A comparison of visual field sensitivity to photoreceptor thickness in retinitis pigmentosa. *Invest Ophthalmol Vis Sci.* 2010;51:4213–4219.
8. Apushkin MA, Alexander KR, Shahidi M. Retinal thickness and visual thresholds measured in patients with retinitis pigmentosa. *Retina.* 2007;27:349–357.
9. Mitamura Y, Aizawa S, Baba T, Hagiwara A, Yamamoto S. Correlation between retinal sensitivity and photoreceptor inner/outer segment junction in patients with retinitis pigmentosa. *Br J Ophthalmol.* 2009;93:126–127.
10. Jacobson SG, Aleman TS, Cideciyan AV, et al. Identifying photoreceptors in blind eyes caused by RPE65 mutations: prerequisite for human gene therapy success. *Proc Natl Acad Sci U S A.* 2005;102: 6177–6182.
11. Hendrickson A, Drucker D. The development of parafoveal and midperipheral human retina. *Behav Brain Res.* 1992;49:21–31.
12. Srinivasan VJ, Monson BK, Wojtkowski M, et al. Characterization of outer retinal morphology with high-speed, ultrahigh-resolution optical coherence tomography. *Invest Ophthalmol Vis Sci.* 2008; 49:1571–1579.
13. Lujan BJ, Roorda A, Knighton RW, Carroll J. Revealing Henle's fiber layer using spectral domain optical coherence tomography. *Invest Ophthalmol Vis Sci.* 2011;52:1486–1492.
14. Curcio CA, Messinger JD, Sloan KR, Mitra A, McGwin G, Spaide RF. Human chorioretinal layer thicknesses measured using macula-wide high resolution histologic sections. *Invest Ophthalmol Vis Sci.* 2011;52:3943–3951.
15. Birch DG, Herman WK, deFaller JM, Disbrow DT, Birch EE. The relationship between rod perimetric thresholds and full-field rod ERGs in retinitis pigmentosa. *Invest Ophthalmol Vis Sci.* 1987;28: 954–965.
16. Barthelmes D, Sutter FK, Kurz-Levin MM, et al. Quantitative analysis of OCT characteristics in patients with achromatopsia and blue-cone monochromatism. *Invest Ophthalmol Vis Sci.* 2006;47: 1161–1166.
17. Thiadens AA, Somervuo V, van den Born LI, et al. Progressive loss of cones in achromatopsia: an imaging study using spectral-domain optical coherence tomography. *Invest Ophthalmol Vis Sci.* 2010; 51:5952–5957.
18. Wald G, Zeavin BH. Rod and cone vision in retinitis pigmentosa. *Am J Ophthalmol.* 1956;42:252–269.
19. Krill AE. *Hereditary and Choroidal Diseases*. New York: Harper and Row; 1972.
20. Massof RW, Finkelstein D. Rod sensitivity relative to cone sensitivity in retinitis pigmentosa. *Invest Ophthalmol Vis Sci.* 1979;18: 263–272.
21. Lyness AL, Ernst W, Quinlan MP, et al. A clinical, psychophysical, and electroretinographic survey of patients with autosomal dominant retinitis pigmentosa. *Br J Ophthalmol.* 1985;69:326–339.
22. Jacobson SG, Voigt WJ, Parel JM, et al. Automated light- and dark-adapted perimetry for evaluating retinitis pigmentosa. *Ophthalmology.* 1986;93:1604–1611.